2016 European Control Conference
June 29 - July 1, 2016. Aalborg, Denmark

Convergence Analysis of Time-Optimal Model Predictive Control under Limited Computational Resources

Christoph Rösmann, Frank Hoffmann and Torsten Bertram

Abstract— **Model predictive control is a means to transit a nonlinear dynamic system from its current towards a target state subject to state and control constraints. A model-predictive controller based on Timed-Elastic-Bands (TEB-MPC) is particular suitable for time-optimal control. This contribution investigates the convergence behavior of the sparse TEB-MPC approach on two non-trivial benchmark systems under limited computational resources. It evaluates the trade-off between accuracy of the approximate optimal solution and computational efficiency. An alternative formulation of the original TEB-MPC with local transition intervals results in a higher dimensional but albeit banded problem structure. Furthermore, both formulations are compared for two different solvers, an unconstrained least-squares optimization and a primary nonlinear program. For low sampling times the former exhibits a faster rate of convergence, however the later is already superior for medium sample times. In practice, the selection of TEB-MPC realizations depends on the order and complexity of the dynamic systems contrasted with the computational resources and demands on real-time control.**

I. INTRODUCTION

Nonlinear model predictive control (MPC) constitutes an advanced control concept for nonlinear system dynamics that considers explicit constraints on control and state variables. Model predictive controllers repeatedly solve a receding horizon optimal control problem within each sampling interval of the underlying feedback control [1]. Solving such optimal control problems under constraints is computationally demanding. In order to utilize MPC for mechatronic systems with fast dynamics the interest in numerical efficient realizations has grown considerably within the past decade.

A major improvement of efficiency and convergence behavior is achieved by the multiple shooting approach [2]. Continuous system dynamics are partitioned into discrete time intervals, for which isolated initial value problems are solved utilizing numerical integration techniques. The calculus of variations is hereby approximated by a sparse finite parameter nonlinear program. To further reduce the computation time, Diehl et al. propose the real-time iteration scheme, which subsequently refines an initial coarse approximation at runtime [3]. The method is based on multiple shooting and involves the computation of only a single (sqp) iteration at each sampling interval. In order to handle stiff systems, implicit integrators are preferred over explicit ones. Recently, lifted integrators based on the inexact newton method are applied to reduce the overall computational cost [4]. D. Kouzoupis combines the real-time iteration scheme with different first-order methods in order to analyze its application to embedded nonlinear MPC [5]. Other methods are based on inner-point-methods that exploit the sparsity of the problem structure in order to allow a numerically efficient computation [6], [7], [8]. Graichen et al. present an efficient method based on projected gradients within a real-time capable MPC scheme [9]. Efficient tailored gradient methods are recently applied to systems governed by partial differential equations [10]. The underlying optimal control problem is transformed into an unconstrained one by means of saturation functions. Other publications focus on automatic code generation strategies that explicitly exploit structure, e.g. in [11] or targeting embedded hardware [12].

In the context of time-optimal MPC, the above mentioned approaches are not generally applicable for real-time applications. Zhao et al. propose an indirect solution based on the calculus of variations to minimize the settling time for quasi time-optimal control of a spherical robot. Indirect methods strongly depend on the initial solution and handling of inequality constraints is difficult in general. An approach that follows a reference path in minimal time is presented in [13]. Time-optimality is nearly achieved in case of sufficiently large time horizons. In applications such as race car automatic control, dedicated MPC methods are utilized in order to minimize the total lap time [14], [15]. Van den Broeck et al. extend the general concept of MPC to time-optimal point-to-point transitions [16]. The method called TOMPC minimizes the settling time in a two layer optimization routine. The outer loop incrementally reduces the horizon of the control sequence until the inner loop nonlinear program fails to generate a feasible solution within the allocated time horizon. The runtime strongly depends on a proper initial estimate of the settling time, as the discrepancy w. r. t. the initial estimate determines the number of iterations in the outer loop time horizon reduction.

Our previous work [17] introduces a novel approach to time-optimal nonlinear MPC for point-to-point transitions. The concept is based on *Timed-Elastic-Bands* (TEB) [18] as a representation of the underlying optimization parameter vector. In contrast to conventional MPC that operate either in continuous time domain or in discrete time domain with a fixed sample rate, the TEB explicitly incorporates the temporal resolution as a parameter of optimization. The continuous system dynamics are approximated by finite differences. This extension enables the efficient minimization of the overall transition time as control and state sequence expand or contract in time and space. A comparative analysis with a state of the art approach and non-trivial benchmark systems

The authors are with the Institute of Control Theory and Systems Engineering, Technische Universität Dortmund, D-44227, Germany, christoph.roesmann@tu-dortmund.de

demonstrates the ability to efficiently refine the planned state and control sequence within the underlying closed-loop control during runtime while converging towards the analytical time-optimal trajectory. In the field of automotive Götte et al. utilize a TEB based MPC approach for the optimal guidance of automated vehicles [19].

The contribution of this paper is twofold. Primarily, two different realizations and extensions of the original time-optimal TEB-MPC problem conducted in [17] are provided that exploit the sparse problem structure. Furthermore, the resulting nonlinear programs are transformed to approximate unconstrained formulations. A comparative convergence analysis of the proposed realizations is performed on two benchmark systems. Although the TEB-MPC approach refines its trajectory during runtime, a fast convergence of the underlying optimal control problem to a feasible suboptimal trajectory is a prerequisite for its successful application. In real world applications the computation time of each feedback interval is either limited by the sampling time or inherent time constants of the plant. Thus, this analysis focuses on the quality of the open-loop solution obtained during the first sampling interval while limiting the computation time to a few milliseconds. Such sample times are common in mechatronic systems. The order of the systems and number of states are of small to medium sizes. Unconstrained variants of TEB-MPC are included in the convergence analysis using penalty functions. Unconstrained optimization does not introduce dual variables thus leading to a smaller problem size. On the other hand the obtained solutions are suspectible w. r. t. weights of the penalty functions. Whether to favor solving unconstrained variants over solving the actual nonlinear programs is revealed by the convergence analysis.

The next section summarizes the original TEB-MPC and introduces an alternative formulation which leads to a modified sparsity pattern with band structure. In Section III both TEB-MPC formulations are transformed into an approximative unconstrained optimization problem. Section IV presents the comparative convergence analysis based on simulations of two benchmark systems. Finally, section V summarizes the results and provides an outlook on further work.

II. Time-Optimal Model Predictive Control

An autonomous, nonlinear dynamic system with p states and q inputs is defined by:

$$\dot{\mathbf{x}}(t) = \mathbf{f}(\mathbf{x}(t), \mathbf{u}(t)), \quad \mathbf{x}(t=0) = \mathbf{x}_s \tag{1}$$

in which $\mathbf{x} \in \mathbb{R}^p$ denotes the time dependent state and $\mathbf{u} \in \mathbb{R}^q$ the corresponding control input. $\mathbf{x}_s \in \mathbb{R}^p$ denotes the initial state at time $t = 0\,\mathrm{s}$. This work utilizes a time-optimal MPC formulation for point-to-point transitions based on *Timed Elastic Bands* (TEB) [17]. Here, the system of differential equations is approximated by finite differences. In contrast to the realization in [17], Crank-Nicolson differences are favored over forward differences to better account for stiff systems:

$$\dot{\mathbf{x}}(t) \approx \frac{\mathbf{x}_{k+1} - \mathbf{x}_k}{\Delta T_k} = \underbrace{0.5\big(\mathbf{f}(\mathbf{x}_k, \mathbf{u}_k) + \mathbf{f}(\mathbf{x}_{k+1}, \mathbf{u}_k)\big)}_{\tilde{\mathbf{f}}(\mathbf{x}_k, \mathbf{x}_{k+1}, \mathbf{u}_k)} \tag{2}$$

The discretization with $k = 0, 1, \ldots, n-1$ introduces n state vectors $\mathbf{x}_k$ and $n-1$ control vectors $\mathbf{u}_k$ according to a sequence of $n-1$ strictly positive time intervals $\Delta T_k \in \mathbb{R}^+$. Two different formulations of the TEB-MPC optimization problem are presented in the following.

A. TEB-MPC Optimization Problem with Global ΔT

The original approach [17] defines a global, uniform time interval $\Delta T_k = \Delta T, \forall k = 1, 2, \ldots, n-1$ between consecutive states and controls. The state sequence, control sequence and the global ΔT are combined into a single set $\mathcal{B}_g \subseteq \mathbb{R}^\rho$ with $\rho = np + (n-1)q + 1$:

$$\mathcal{B}_g := \{\mathbf{x}_1, \mathbf{u}_1, \mathbf{x}_2, \mathbf{u}_2, \ldots, \mathbf{x}_{n-1}, \mathbf{u}_{n-1}, \mathbf{x}_n, \Delta T\} \tag{3}$$

The control task involves the transition from the initial state $\mathbf{x}_s$ to a final target state $\mathbf{x}_f$ in minimum time T. Since the TEB-MPC explicitly incorporates the time interval ΔT as part of the optimization, the transition time in terms of the parameter set $\mathcal{B}_g$ is given by $T \approx (n-1)\Delta T$. The optimal control sequence is obtained by solving the nonlinear program consisting of the linear objective function $V_g(\mathcal{B}_g) = (n-1)\Delta T$ that is bounded from below due to a strictly positive ΔT:

$$V_l^*(\mathcal{B}_g) = \min_{\mathcal{B}_g} \quad (n-1)\Delta T \tag{TEB$_g$}$$

subject to

$$\begin{aligned}
&\mathbf{x}_1 = \mathbf{x}_s, \quad \mathbf{x}_n = \mathbf{x}_f, \quad 0 < \Delta T \leq \Delta T_{max} \\
&\mathbf{h}_k(\mathbf{x}_{k+1}, \mathbf{x}_k, \mathbf{u}_k, \Delta T) = \mathbf{0} \\
&\mathbf{g}_k(\mathbf{x}_k, \mathbf{u}_k) \geq \mathbf{0} \qquad\qquad (k = 1, 2, \ldots, n-1)
\end{aligned}$$

Initial and final states, $\mathbf{x}_1$ and $\mathbf{x}_n$, are clipped to the actual start and goal state vector $\mathbf{x}_s$ and $\mathbf{x}_f$ respectively. System dynamics are incorporated by the following equality constraint:

$$\mathbf{h}_k(\mathbf{x}_{k+1}, \mathbf{x}_k, \mathbf{u}_k, \Delta T) = \frac{\mathbf{x}_{k+1} - \mathbf{x}_k}{\Delta T_k} - \tilde{\mathbf{f}}(\mathbf{x}_k, \mathbf{x}_{k+1}, \mathbf{u}_k) \tag{4}$$

States and controls are restricted by inequality constraints $\mathbf{g}_k : \mathbb{R}^p \times \mathbb{R}^q \to \mathbb{R}^r$. ΔT_{max} denotes an upper bound on the discretization width which is usually chosen to be compliant with the sampling theorem.

Notice, in case of a fixed ΔT during optimization, the finite difference approximation is easily transformed into numerical integration and thus constitutes a multiple shooting approach. However, in our experience performing numerical integration with a non-fixed ΔT appears to result in a less robust convergence. Additionally, the finite differences formulation introduces an implicit barrier on ΔT forcing it to be strictly positive since the difference quotient diverges for $\Delta T \to 0$.

B. TEB-MPC Optimization Problem with Local ΔT_k

A global ΔT shared among all state transitions introduces a dense row and column in the Hessian matrix of the optimization problem since the discrete system dynamics of all states depend on the very same parameter ΔT. An alternative structure is achieved by maintaining separate time intervals ΔT_k that are local to each state. The sequences of states, controls and time intervals are combined into a single set $\mathcal{B}_l \subseteq \mathbb{R}^{\varrho}$ with $\varrho = np + (n-1)(q+1)$:

$$\mathcal{B}_l := \{\mathbf{x}_1, \mathbf{u}_1, \Delta T_1, \mathbf{x}_2, \mathbf{u}_2, \Delta T_2, \ldots, \mathbf{x}_{n-1}, \mathbf{u}_{n-1}, \Delta T_{n-1}, \mathbf{x}_n\} \quad (5)$$

The optimal control sequence is obtained by solving the following nonlinear program:

$$V_g^*(\mathcal{B}_l) = \min_{\mathcal{B}_l} \sum_{k=1}^{n-1} \Delta T_k^2 \quad (\text{TEB}_l)$$

subject to

$$\begin{aligned} &\mathbf{x}_1 = \mathbf{x}_s, \quad \mathbf{x}_n = \mathbf{x}_f, \quad 0 < \Delta T_k \leq \Delta T_{max} \\ &\mathbf{h}_k(\mathbf{x}_{k+1}, \mathbf{x}_k, \mathbf{u}_k, \Delta T_k) = \mathbf{0} \\ &\mathbf{g}_k(\mathbf{x}_k, \mathbf{u}_k) \geq \mathbf{0} \qquad (k = 1, 2, \ldots, n-1) \end{aligned}$$

The original objective function $V_g(\mathcal{B}_g)$ is replaced by the sum of squared time intervals. Notice, that the total transition time is approximated by $T \approx \sum_{i=0}^{n-1} \Delta T_k$. The resulting nonlinear program is underconstrained as the total time T can be partitioned in different ways into the individual summands ΔT_k. This ambiguity is resolved by (TEB_l) as the squared terms ΔT_k^2 favor a uniform interval $\Delta T_k^* \approx \frac{T}{n}$.

C. Solving the TEB-MPC Optimization Problem

The solution of (TEB_g) and (TEB_l) is obtained by applying constrained optimization algorithms for which several alternative numerical software packages are readily available. The IPOPT software package employs interior point methods [20], it is particular suitable for sparse nonlinear programs, supports warm starts and is written in C++. The selected sparse linear solver HSL-MA57 [21] is targeted for small and medium sized problems. The solver depends on Jacobian matrices for the objective function and constraints as well as the Hessian of the Lagrangian. For the evaluation part IPOPT is fed with numerically calculated Jacobian and Hessian matrices to avoid convergence effects that tend to emerge in iterative BFGS methods [22]. In order to take advantage of the sparsity structure for calculating the Jacobians and Hessian, the complete nonlinear program is represented as a hyper-graph which vertices denote optimization parameters in $\mathcal{B}_l$ resp. $\mathcal{B}_g$ and which edges denote the constraints $\mathbf{h}_k$, $\mathbf{g}_k$ as well as the summands of the objective functions. Each edge depends only on a small subset of the entire set of TEB parameters. Dense block Jacobian and Hessian submatrices are computed numerically with finite differences by iterating through all edges of the graph. Those submatrices of edges that correspond to linear or quadratic terms are defined in analytical form. Finally all submatrices are combined into the overall sparse Jacobian resp. Hessian matrices.

D. Closed-Loop Control

Closed-loop control with TEB-MPC is described in [17]. The following algorithm details the basic approach:

```
procedure TEBMPC(B, x_s, x_f)
    Initialize or update trajectory
    for all Iterations 1 to I_teb do
        Adjust length n of the trajectory
        B* ← SOLVENLP(B)            ▷ (TEB_g) or (TEB_l)
        Check feasibility
    return (sub-) optimal B*, u*_1
```

At the beginning of each feedback sampling interval, state and control sequences are updated according to the current state $\mathbf{x}_s$ or to a novel final state $\mathbf{x}_f$. Sequences obtained from previous optimizations $\mathcal{B}$ are reutilized as for initialization to enable warm starting. The initial state sequence is obtained from linear interpolation between current and final state with zero controls. A dedicated loop with I_{teb} cycles sequentially adjusts the length n of the state and control sequences. The purpose of this adaptation is to adapt the TEB length towards a reference discretization interval ΔT_{ref} by inserting or deleting samples. Even with a poor guess of the initial trajectory length, the TEB converges rapidly towards the optimal state sequence. In case of (TEB_g) the entire trajectory is resampled using linear interpolation, see [17] for details. Regarding (TEB_l), it is sufficient to find the first ΔT_k for which $|\Delta T_k - \Delta T_{ref}| < \epsilon$ is violated and either remove or add a new sample using linear interpolation. Finally, the nonlinear program is solved. After I_{teb} iterations the first optimal control input $\mathbf{u}_1^*$ is applied to the plant.

Remarks on optimality and stability of the TEB approach are provided in [17]. This work focuses on point-to-point transitions towards a fixed goal state which requires a decreasing objective function within consecutive sampling intervals while retaining feasibility. In practice time optimal controllers are not favored for stabilizing control, such that in the vicinity of the target state the MPC (softly) switches to a conventional quadratic cost function.

III. APPROXIMATE UNCONSTRAINED OPTIMIZATION

This paper further investigates the application of unconstrained optimization techniques to the time-optimal TEB-MPC approach that support sparsity patterns and approximate the original nonlinear programs (TEB_g) and (TEB_l). Unconstrained optimization avoids Lagrange/KKT multipliers causing the dimension of the Hessian matrices to become identical with the number of primary variables in $\mathcal{B}_g$ resp. $\mathcal{B}_l$. On the other hand, handling hard constraints is difficult.

The nonlinear least-squares optimization problem is solved efficiently as the solver approximates the Hessian from first order derivatives. This approximation requires that the unconstrained objective function is composed of squared nonlinear terms only. Quadratic penalty functions are applied to constraints according to [22]. Notice, that other approximations like barrier, augmented Lagrangian or exact penalty methods [23] exist, which however contain terms that are not destined to be squared and can therefore not be applicated here. In the following, the transformation is presented based on the nonlinear program (TEB$_g$). The transformation applies directly to (TEB$_l$) by substituting subscripts g by l if not stated otherwise.

A. Nonlinear Least-Squares Approximation with Penalties

The equality constraints are expressed by quadratic penalty functions. For the sake of readability arguments of constraints are omitted in the following:

$$\phi(\mathbf{h}_k, \sigma_1) = \sigma_1 \mathbf{h}_k^\intercal \mathbf{I} \mathbf{h}_k = \sigma_1 ||\mathbf{h}_k||_2^2 \tag{6}$$

σ_1 denotes a scalar weight and $\mathbf{I} \in \mathbb{R}^{p \times p}$ is the identity matrix. Inequality constraints are approximated by the following quadratic penalty function:

$$\chi(\mathbf{g}_k, \sigma_2) = \sigma_2 || \min\{[\mathbf{0}, \mathbf{g}_k(\mathbf{x}_k, \mathbf{u}_k)]\}||_2^2 \tag{7}$$

Here, the min-operator is applied row-wise. σ_2 denotes a scalar weight. Constraints $\mathbf{x}_1 = \mathbf{x}_s$ and $\mathbf{x}_n = \mathbf{x}_f$ are eliminated by substitution and are therefore not subject to the optimization. ΔT is implicitly bounded to $\mathbb{R}^+$ due to the difference quotient in (2) and a positive initial value as stated in section II-A. With (6) and (7) the approximative, unconstrained optimization problem is defined as follows:

$$\mathcal{B}_g^* = \operatorname*{arg\,min}_{\mathcal{B}_g \setminus \{\mathbf{x}_1, \mathbf{x}_n\}} V_g^2(\mathcal{B}_g) + \sum_{k=0}^{n-1} \big[\phi(\mathbf{h}_k, \sigma_1) + \chi(\mathbf{g}_k, \sigma_2)\big] \tag{8}$$

Squaring the original objective function $V_g(\mathcal{B}_g)$ does not change the minimizer of (TEB$_g$), since ΔT is strictly positive by definition. In case of (TEB$_l$), $V_l(\mathcal{B}_l)$ already constitutes a least-squares objective and requires no squared form.

Transforming nonlinear programs into equivalent unconstrained optimization problems is a common procedure and the minimizer of (8) coincides with the actual minimizer of (TEB$_g$) only if $\sigma_{1,2} \rightarrow \infty$ [22]. However, large weights introduce ill-conditioned properties and therefore the underlying solver does not accept adequate step sizes. The problem might not converge properly. A common remedy is to increase σ_1 and σ_2 successively with each iteration. Regarding our benchmark systems, initializing $\sigma_1 = \sigma_2 = 2$ in each feedback sampling interval and adapting them according to $\sigma^{(i+1)} = \kappa \sigma^{(i)}$ with $\kappa = 1.2$ at each loop of the TEB-MPC algorithm (see Section II-C) performs well. Since the MPC is integrated with state feedback and therefore refines its trajectory during runtime, the actual minimizer for $\sigma_{1,2} \rightarrow \infty$ is waived in exchange for a suboptimal but more efficient solution.

B. Solution of the Unconstrained Problem

The literature reports many solvers for nonlinear least-squares problems (8) such as the popular Gauss-Newton or Levenberg-Marquardt (LM) algorithm [22]. Our approach employs LM due to its proper balance between robustness and efficiency. LM constitutes a trust-region strategy that only accepts step sizes that decrease the overall cost. Applying the approach requires the solution of a sparse linear system for which $(\mathbf{H}+\lambda\mathbf{I})^{-1}$ is computed. $\mathbf{H} = \mathbf{J}^\intercal\mathbf{J}$ denotes

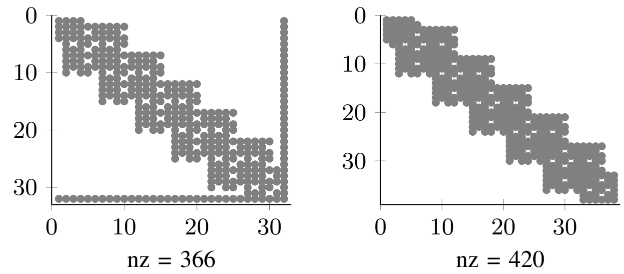

(a) Global ΔT (b) Local ΔT_k

Fig. 1: Hessian matrices of the coupled van-der-pol oscillator.

the Hessian that itself depends on the Jacobian $\mathbf{J}$. λ denotes a damping factor. The implemented algorithm is borrowed from [24]. The Jacobian $\mathbf{J}$ is represented as a sparse matrix and is composed from a hyper-graph with dense block Jacobians as described above. A direct *LLt* cholesky factorization with fill-in reducing is utilized as sparse linear solver which is available as part of the C++ math library *Eigen* [25]. Hessian matrix structures of both least-squares approximations (global and local ΔT) are shown in Figure 1.

IV. Convergence Analysis and Examples

This section analyzes the convergence behavior under limited computational resources by comparing the different realizations of the MPC-TEB controller in simulation. It investigates the solution of the open-loop optimal control problem within the very first sampling interval. In this case, a simple and coarse initial trajectory is optimized, while in further feedback sampling intervals previously obtained solutions are updated and re-optimized (warm starting). Due to this fact the quality of the first solution is crucial for the overall control accuracy. In order to analyze and compare the convergence resp. optimality of each state or control sequence, the normalized root-mean-square error (NRMSE) of both sequences obtained from open-loop control w.r.t. to the known optimal solution is observed. Applying open-loop control with the same plant model in simulation enforces satisfaction of constraints. The optimal solution is obtained by solving the nonlinear program (TEB$_g$) of the TEB-MPC approach, whose optimality has been validated on other benchmark systems in [17]. The reference nonlinear program converges towards a KKT point and therefore satisfies first order necessary conditions for optimality. Notice, that measuring the NRMSE rather than the residual error towards the KKT-Point is favored, since the approximative objective function (8) does not contain necessary Lagrange multipliers and it further allows a more intuitive interpretation than artificial merit function values. Simulations are performed in C++ running on Ubuntu 14.04 (PC: 3.4 GHz Intel i7 CPU).

A. Coupled Van-der-Pol Oscillator

The first benchmark system is composed of two coupled Van-der-Pol oscillators. Each Van-der-Pol oscillator in its own constitutes a second order system with nonlinear damping. The coupled system is defined by the following nonlinear differential equations.

$$\ddot{x}_1 = -(x_1^2 - 1)\dot{x}_1 - x_1 + (x_2 - x_1) + u \quad (9)$$
$$\ddot{x}_2 = -(x_2^2 - 1)\dot{x}_2 - x_2 + (x_1 - x_2) \quad (10)$$

Only the first oscillator is effected by the control input u. Transforming these equations into a state space representation with state vector $\mathbf{x} = [x_1, \dot{x}_1, x_2, \dot{x}_2]^\intercal$ results in a fourth order system:

$$\dot{\mathbf{x}} = \mathbf{f}(\mathbf{x}, u) = \begin{bmatrix} \dot{x}_1 \\ -(x_1^2 - 1)\dot{x}_1 - 2x_1 + x_2 + u \\ \dot{x}_2 \\ -(x_2^2 - 1)\dot{x}_2 - 2x_2 + x_1 \end{bmatrix} \quad (11)$$

The control task is to guide the system from the initial state $\mathbf{x}_0 = \mathbf{0}$ towards the final state $\mathbf{x}_f = [1, 0, 0.5, 0]^\intercal$ in minimal time while restricting the control to $|u| \leq 1.6$. Equality constraints $\mathbf{h}_k$ are obtained by combining (4) with (2) and (11). Bounds on u are captured by $\mathbf{g}_k(u_k) = [u + 1.6, -u + 1.6]^\intercal$. In the following analysis the computation time for optimization is bounded to $25\,\mathrm{ms}$ while the trajectory length n is varied. The resulting NRMSE for the different approaches

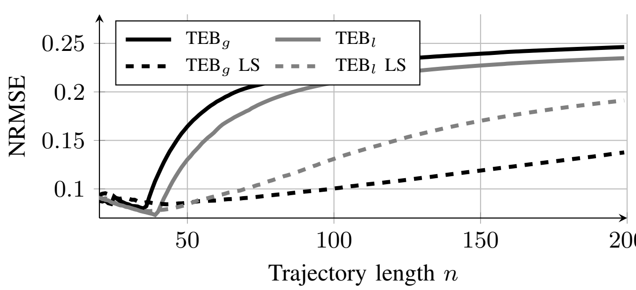

Fig. 2: Open-Loop control result with fixed computation time to $25\,\mathrm{ms}$ and increasing trajectory length n

w.r.t. reference state and control sequences is depicted in Figure 2. Two different phases in the evolution of the NRME over the trajectory length are apparent. In the first phase ($n < 50$) the error decreases as the discretization error w.r.t. to the optimal solution with $n = 200$ is reduced with more samples. The TEB optimizations converge within the first $25\,\mathrm{ms}$. Even at a resolution of $n < 50$ a fit of more than 90% is achieved. The fit is calculated by $100(1 - NRMSE)\%$. In the second phase ($n > 50$) the optimizer is no longer able to converge within the first $25\,\mathrm{ms}$. As the computational burden increases with the number of parameters the convergence deteriorates for increasing trajectory length. The least-squares (LS) realizations of TEB-MPC generally exhibit lower errors, whereas (TEB$_g$) performs best. Global ΔT approaches score better on this benchmark. Figure 3 shows the evolution of the NRMSE for $n = 70$ w.r.t. the elapsed computation time in this ignoring the $25\,\mathrm{ms}$ restriction. Obviously, the least-squares realizations converge faster to a suboptimal solution of 90% fit than the original nonlinear programs. However, beyond a computational budget of $50\,\mathrm{ms}$, the actual programs outperform the least-squares solutions that converge more slowly to the optimal solution. Notice, that the NRME is still

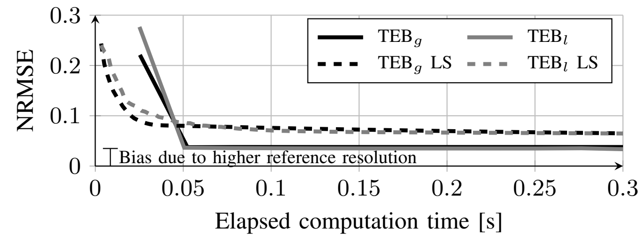

Fig. 3: Convergence of the Coupled-Van-der-Pol oscillator

biased, since the reference solution has a higher resolution ($n = 200$) with steeper steps in the control. Reference state and control trajectories are depicted in Figure 4. Figure 4

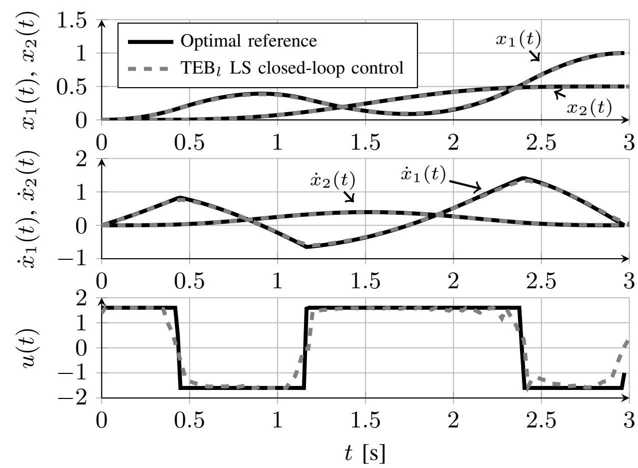

Fig. 4: Reference trajectories and closed-loop example

also shows an example of the closed-loop control achieved by the least-squares approximation with local ΔT_k. It copes with a slight model mismatch due to a 5th order Runge-Kutta integrator in the actual plant model.

B. Integrator Chain with State and Input Nonlinearities

The second benchmark analyzes the evolution of the NRMSE w.r.t. an increasing state vector dimension p leading to larger dense blocks in the Hessian (see Figure 1). In particular, the benchmark system models a chain of p integrator systems with input nonlinearities. The overall system is defined with $\mathbf{x} = [x_1, x_2, \ldots, x_p]^\intercal$ as follows:

$$\dot{\mathbf{x}} = \mathbf{f}(\mathbf{x}, u) = \begin{bmatrix} \tanh(x_2) \\ \tanh(x_3) \\ \vdots \\ \tanh(x_p) \\ \tanh(u) \end{bmatrix} \quad (12)$$

The control task is the transition between $\mathbf{x}_s = \mathbf{0}$ and $\mathbf{x}_f = [1, 0, 0, \ldots]^\intercal$ in minimal time with $|u| \leq 1$. Computational resources for the MPC step are limited to $10\,\mathrm{ms}$. Trajectory lengths are fixed to $n = 50$. Figure 5 depicts the evolution of the NRMSE w.r.t. system order p for the different TEB-MPC realizations. For each order p, reference state and control sequences are generated according to the previous example with resolution $n = 50$. The evolution of (TEB$_g$) and (TEB$_l$)

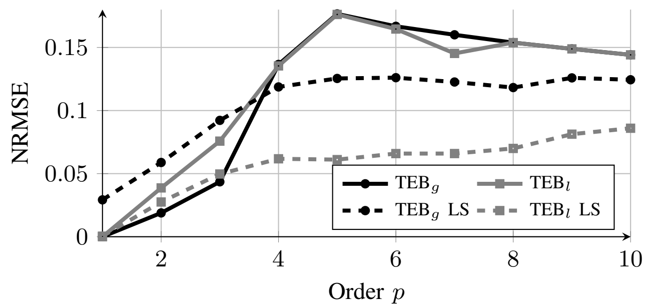

Fig. 5: Integrator system with increasing order: open-loop solution after $10\,\text{ms}$ computation time.

is similar to each other. Like in the previous benchmark, the least-squares approximations are able to achieve a lower NRMSE (in particular for $p \geq 4$) within the first $10\,\text{ms}$, but apparently the local ΔT_k approach performs best on this benchmark. This might be caused by the growth of the local structure (dense blocks for each tuple $\{\mathbf{x}_k, \mathbf{x}_{k+1}, \mathbf{u}, \Delta T_k\}$) of the Hessian that mostly depend on the system dynamics constraint with dimension p. The local approach does not share a common ΔT which requires global adaptation across all state transitions.

V. CONCLUSIONS AND FUTURE WORK

The TEB-MPC formulation for time-optimal point-to-point transitions is extended to an alternative representation resulting in a banded sparsity pattern. Under limited computational resources, a convergence investigation is performed on two different benchmark systems. In particular, the problem size is varied either by increasing the trajectory resolution and or by increasing the order of the system dynamics. Least-squares approximations of the optimization problem are applied to the original problems and are included in the evaluation. It turns out that they provide an approximate solution that matches nearly $90\,\%$ of the optimal solution within a very short computation time. Surprisingly, solving the actual TEB-MPC nonlinear programs is fast, such that they quickly converge towards a nearby perfect match. As a conclusion solving the constrained problem is favorable as long as the computational resources are sufficient. In applications that are restricted to tight computational budgets, the least-squares solution provides a reasonable trade-off between efficiency and optimality. As a second insight, the banded sparsity pattern performs better for higher order systems whereas the original approach provides a better solution in case of the first benchmark system and a much higher resolution. In practice, the decision for either one of the approaches might depends on the specific properties of the system and the real-time demands of the application.

Future work is concerned with the generalization of the results within a theoretical framework. In order to close the gap between the least-squares solution and the actual KKT-point, more advanced penalty adaptation methods are considered. Furthermore, the newly introduced sparsity pattern constitutes a banded matrix for which dedicated solvers might be utilized.

REFERENCES

[1] M. Morari and J. H. Lee, "Model predictive control: past, present and future," *Computers & Chemical Engineering*, vol. 23, no. 4-5, pp. 667–682, 1999.

[2] M. Diehl, H. G. Bock, J. P. Schlöder, R. Findeisen, Z. Nagy, and F. Allgöwer, "Real-time optimization and nonlinear model predictive control of processes governed by differential-algebraic equations," *Journal of Process Control*, vol. 12, no. 4, pp. 577–585, 2002.

[3] M. Diehl, H. G. Bock, and J. P. Schlöder, "A real-time iteration scheme for nonlinear optimization in optimal feedback control," *SIAM Journal on Control and Optimization*, vol. 43, no. 5, pp. 1714–1736, 2005.

[4] R. Quirynen, S. Gros, and M. Diehl, "Inexact newton based lifted implicit integrators for fast nonlinear mpc," in *IFAC Nonlinear Model Predictive Control Conference (NMPC)*, 2015.

[5] D. Kouzoupis, H. J. Ferreau, and M. Diehl, "First-order methods in embedded nonlinear model predictive control," in *European Control Conference (ECC)*, 2015.

[6] Y. Wang and S. P. Boyd, "Fast model predictive control using online optimization," in *IFAC World Congress*, vol. 17, 2008, pp. 6974–6979.

[7] A. Richards, "Fast model predictive control with soft constraints," in *European Control Conference*, 2013, pp. 1–6.

[8] K. S. Pakazad, H. Ohlsson, and L. Ljung, "Sparse control using sum-of-norms regularized model predictive control," in *IEEE Conference on Decision and Control*, 2013.

[9] K. Graichen and B. Käpernick, "A real-time gradient method for nonlinear model predictive control," in *Frontiers of Model Predictive Control*, 2012.

[10] S. Rhein, T. Utz, and K. Graichen, "Efficient state constraint handling for mpc of the heat equation," in *UKACC International Conference on Control*, 2014.

[11] M. Vukov, A. Domahidi, H. J. Ferreau, M. Morari, and M. Diehl, "Auto-generated algorithms for nonlinear model predictive control on long and on short horizons," in *IEEE Annual Conference on Decision and Control*, 2013, pp. 5113–5118.

[12] D. K. M. Kufoalor, B. J. T. Binder, H. J. Ferreau, L. Imsland, T. A. Johanse, and M. Diehl, "Automatic deployment of industrial embedded model predictive control using qpoases," in *European Control Conference (ECC)*, 2015.

[13] D. Lam, "A model predictive approach to optimal path-following and contouring control," PhD Thesis, The University of Melbourne, 2012.

[14] D. P. Kelly and R. S. Sharp, "Time-optimal control of the race car: a numerical method to emulate the ideal driver," *Vehicle System Dynamics*, vol. 48, no. 12, pp. 1461–1474, 2010.

[15] J. P. Timings and D. J. Cole, "Minimum manoeuvre time of a nonlinear vehicle at constant forward speed using convex optimisation," in *International Symposium on Advanced Vehicle Control*, 2010.

[16] L. Van den Broeck, M. Diehl, and J. Swevers, "A model predictive control approach for time optimal point-to-point motion control," *Mechatronics*, vol. 21, no. 7, pp. 1203–1212, 2011.

[17] C. Rösmann, F. Hoffmann, and T. Bertram, "Timed-elastic-bands for time-optimal point-to-point nonlinear model predictive control," in *European Control Conference (ECC)*, 2015.

[18] C. Rösmann, W. Feiten, T. Wösch, F. Hoffmann, and T. Bertram, "Efficient trajectory optimization using a sparse model," in *European Conference on Mobile Robots*, 2013, pp. 138–143.

[19] C. Götte, M. Keller, C. Haß, K.-H. Glander, A. Seewald, and T. Bertram, "A model predictive combined planning and control approach for guidance of automated vehicles," in *IEEE International Conference on Vehicular Electronics and Safety*, 2015.

[20] A. Wächter and L. T. Biegler, "On the implementation of a primal-dual interior point filter line search algorithm for large-scale nonlinear programming," *Mathematical Programming*, vol. 106, no. 1, pp. 25–57, 2006.

[21] "HSL. A collection of Fortran codes for large scale scientific computation." [Online]. Available: http://www.hsl.rl.ac.uk/

[22] J. Nocedal and S. J. Wright, *Numerical optimization*, ser. Springer series in operations research. New York: Springer, 1999.

[23] E. C. Kerrigan and J. M. Maciejowski, "Soft constraints and exact penalty functions in model predictive control," in *UKACC International Conference*, Cambridge and UK, 2000.

[24] M. A. Lourakis and A. Argyros, "SBA: A software package for generic sparse bundle adjustment," *ACM Trans. Math. Software*, vol. 36, no. 1, pp. 2:1–2:30, 2009.

[25] G. Guennebaud and B. Jacob, "Eigen v3," 2010. [Online]. Available: http://eigen.tuxfamily.org